JYX
JYVÄSKYLÄN YLIOPISTO
UNIVERSITY OF JYVÄSKYLÄ

This is a self-archived version of an original article. This version may differ from the original in pagination and typographic details.

Author(s): Kostensalo, Joel; Suhonen, Jouni

Title: Consistent large-scale shell-model analysis of the two-neutrino ββ and single β branchings in 48Ca and 96Zr

Year: 2020

Version: Published version

Copyright: © 2019 The Author(s)

Rights: CC BY 4.0

Rights url: https://creativecommons.org/licenses/by/4.0/

Please cite the original version:

Kostensalo, J., & Suhonen, J. (2020). Consistent large-scale shell-model analysis of the two-neutrino ββ and single β branchings in 48Ca and 96Zr. Physics Letters B, 802, Article 135192. https://doi.org/10.1016/j.physletb.2019.135192

Physics Letters B 802 (2020) 135192

Contents lists available at ScienceDirect

Physics Letters B

www.elsevier.com/locate/physletb

Consistent large-scale shell-model analysis of the two-neutrino $\beta\beta$ and single β branchings in ^{48}Ca and ^{96}Zr

Joel Kostensalo *, Jouni Suhonen

University of Jyvaskyla, Department of Physics, P. O. Box 35, FI-40014, Finland

ARTICLE INFO

Article history:
Received 20 August 2019
Received in revised form 20 December 2019
Accepted 23 December 2019
Available online 3 January 2020
Editor: W. Haxton

Keywords:
Double-beta decay
Axial-vector coupling
^{48}Ca
^{96}Zr
Shell model
Matrix elements

ABSTRACT

Two-neutrino double-beta-decay matrix elements $M_{2\nu}$ and single beta-decay branching ratios were calculated for ^{48}Ca and ^{96}Zr in the interacting nuclear shell model using large single-particle valence spaces with well-tested two-body Hamiltonians. For ^{48}Ca the matrix element $M_{2\nu} = 0.0511$ is obtained, which is 5.5% smaller than the previously reported value of 0.0539. For ^{96}Zr this work reports the first large-scale shell-model calculation of the nuclear matrix element, yielding a value $M_{2\nu} = 0.0747$ with extreme single-state dominance. These matrix elements, combined with the available $\beta\beta$-decay half-life data, yield effective values of the weak axial coupling which in turn are used to produce in a consistent way the β-decay branching ratios of (7.5 ± 2.8)% for ^{48}Ca and (18.4 ± 0.09)% for ^{96}Zr. These are larger than obtained in previous studies, implying that the detection of the β-decay branches could be possible in dedicated experiments sometime in the (near) future.

© 2019 The Author(s). Published by Elsevier B.V. This is an open access article under the CC BY license (http://creativecommons.org/licenses/by/4.0/). Funded by SCOAP^3.

The nuclei ^{48}Ca and ^{96}Zr share an interesting feature, the two being the only known nuclei where single β-decay transitions compete with the dominant two-neutrino double beta ($2\nu\beta\beta$) decay [1]. This exceptional situation is due to the large angular-momentum difference ($\Delta J = 4, 5, 6$) between the initial and final states of β decays, as well as the relatively small decay energies (Q values). Both theoretical and experimental studies have been carried out regarding decays of both nuclei [2–8]. The two-neutrino-emitting modes are dominated by the ground-state-to-ground-state transitions with resent half-life estimates of $6.4^{+1.4}_{-1.1}$ for ^{48}Ca [9] and 2.35 ± 0.21 for ^{96}Zr [10]. These two nuclei are favorable for experimental double-beta-decay studies due to their large Q values: ^{48}Ca having the largest known double-β Q value $Q_{\beta\beta}(^{48}\text{Ca}) = 4269.08(8)$ keV, and ^{96}Zr having the third largest value $Q_{\beta\beta}(^{96}\text{Zr}) = 3356.03(7)$ keV, with only ^{150}Nd between them [11].

The single-β channels have not yet been observed but lower limits for the half-lives stand at 1.1×10^{20} yr for ^{48}Ca [5] and 2.6×10^{19} yr for ^{96}Zr [12]. Were these observed, they would provide valuable information about the validity of current nuclear models, which could be used to improve the accuracy of calculations of the matrix elements of neutrinoless $\beta\beta$ decay.

In this Letter we revisit the previous theoretical studies, giving an updated estimate for the $2\nu\beta\beta$-decay matrix element for ^{48}Ca and for the first time a shell-model estimate for the ^{96}Zr $2\nu\beta\beta$-decay matrix element. Using this information we present improved estimates for the β-decay branching ratios. This knowledge can in the future be used to design optimal experiments for the detection of the β-decay branches.

The theory of β decay, including the forbidden transitions considered here, is extensively treated in the work of Behrens and Bühring [13]. A streamlined presentation of the theory, including all the technical details of how the calculations were carried out also in the present work, can be found from [14]. The basic theory behind the $2\nu\beta\beta$ decay can be found in much more detail for example from [15].

For β decay the probability of the electron being emitted with kinetic energy between W_e and $W_e + dW_e$ is

$$P(W_e)dW_e = \frac{G_F}{(\hbar c)^6}\frac{1}{2\pi^3\hbar}C(W_e) \times p_e c W_e (W_0 - W_e)^2 F_0(Z, W_e) dW_e, \quad (1)$$

where p_e is the momentum of the electron, Z is the proton number of the final-state nucleus, $F_0(Z, W_e)$ is the so-called Fermi function, and W_0 is the end-point energy of the β spectrum. The nuclear-structure information is encoded as form factors in the shape factor $C(w_e)$. In the impulse approximation, where we assume that the decaying nucleon does not interact with the other

* Corresponding author.
E-mail address: joel.j.koatensalo@student.jyu.fi (J. Kostensalo).

https://doi.org/10.1016/j.physletb.2019.135192
0370-2693/© 2019 The Author(s). Published by Elsevier B.V. This is an open access article under the CC BY license (http://creativecommons.org/licenses/by/4.0/). Funded by SCOAP^3.

$A-1$ nucleons at the moment of decay, these form factors map to nuclear matrix elements (NMEs), which can in turn be calculated using a many-body framework, such as the interacting nuclear shell model. The axial-vector coupling g_A and the vector coupling g_V, which enter the theory of β decay when the vector and axial-vector hadronic currents become renormalized at the nucleon level, appear as multipliers of the various axial-vector and vector matrix elements respectively.

The half-life of β decay can be written as

$$t_{1/2} = \frac{\kappa}{\tilde{C}}, \tag{2}$$

where $\tilde{C}$ is the integrated shape function and the constant κ has the value [16]

$$\kappa = \frac{2\pi^3\hbar^7 \ln 2}{m_e^5 c^4 (G_F \cos\theta_C)^2} = 6147 \text{ s}, \tag{3}$$

θ_C being the Cabibbo angle. To simplify the formalism it is traditional to introduce unitless kinematic quantities $w_e = W_e/m_e c^2$, $w_0 = W_0/m_e c^2$ and $p = p_e c/(m_e c^2) = \sqrt{w_e^2 - 1}$, and so the integrated shape function can then be expressed as

$$\tilde{C} = \int_1^{w_0} C(w_e) p w_e (w_0 - w_e)^2 F_0(Z, w_e) dw_e. \tag{4}$$

The shape factor $C(w_e)$ of Eq. (4) contains complicated combinations of both (universal) kinematic factors and NMEs. As in the previous studies regarding forbidden β decays [14,17,18] we take into account the next-to-leading-order terms of the shape factor as well as screening and radiative effects.

For the $2\nu\beta\beta$ decay the half-life expression is analogous to that of β decay in Eq. (2) and can be written as [15]

$$t_{1/2}^{(2\nu)} = \frac{1}{G^{(2\nu)} g_A^4 |M_{2\nu}|^2}, \tag{5}$$

where $G^{(2\nu)}$ is the phase-space integral (the expression for this is given in, e.g. [15]) and $M_{2\nu}$ is the matrix element given for $\beta^-\beta^-$ decay by

$$M_{2\nu} = \sum_m \frac{(0_{\text{g.s.}}^{(f)} || \sigma\tau^- || 1_m^+)(1_m^+ || \sigma\tau^- || 0_{\text{g.s.}}^{(i)})}{[\frac{1}{2} Q_{\beta\beta} + E(1_m^+) - M_i]/m_e + 1}, \tag{6}$$

where m_e is the electron rest mass, $E(1_m^+) - M_i$ is the energy difference between the mth intermediate 1^+ state and the ground state of the initial nucleus, and $Q_{\beta\beta}$ is the energy released in the decay (i.e. Q value).

The nuclear-structure calculations were done using the interacting shell model with the computer code NuShellX@MSU [19]. Following the earlier shell-model studies regarding the half-lives of the transitions $^{48}\text{Ca}(0^+) \to {}^{48}\text{Sc}(4^+, 5^+, 6^+)$ [6] and the $2\nu\beta\beta$-decay channel [20], the full fp model space with the interaction GXPF1A [21,22] was used.

For the decay of ^{96}Zr a model space including the proton orbitals $0f_{5/2}$, $1p_{3/2}$, $1p_{1/2}$ and $0g_{9/2}$ and the neutron orbitals $0g_{7/2}$ $1d_{5/2}$, $1d_{3/2}$ and $2s_{1/2}$ were used together with the interaction glekpn [23]. In the previous shell-model study [8] the calculations were done in the much smaller proton $0g_{9/2}$–$1p_{1/2}$ and neutron $1d_{5/2}$–$2s_{1/2}$ model space with the Gloeckner interaction [24]. While the exclusion of a large number of important orbitals can affect the accuracy of the computed half-lives of the various β-decay branches, the problem is even more severe for the ground-state-to-ground-state $2\nu\beta\beta$ decay, which is strictly forbidden in such a limited model space. In the present study this transition can proceed by simultaneous Gamow-Teller transitions between the proton $0g_{9/2}$ and neutron $0g_{7/2}$ orbitals.

Table 1
Shell-model calculated $2\nu\beta\beta$ NMEs and the extracted effective value g_A^{eff} of the axial-vector coupling.

Nucleus	$\lvert M_{2\nu}\rvert$	G (10^{-18} yr^{-1}) [25]	$T_{1/2}^{\beta\beta}$ (10^{19} yr)	g_A^{eff}
^{48}Ca	0.0511	14.805	$6.4^{+1.4}_{-1.1}$ [9]	0.80 ± 0.04
^{96}Zr	0.0747	6.420	2.35 ± 0.21 [10]	$1.04^{+0.03}_{-0.02}$

Since the computational burden for description of these decays is manageable for modern computers, we included all the intermediate 1^+ states of $2\nu\beta\beta$ decay in ^{48}Sc and ^{96}Nb. This is an improvement over the previous calculation regarding the matrix element of ^{48}Ca [20], where only 250 intermediate states were used. For ^{48}Sc our extended calculation includes 9470 1^+ states and excitation energies up to 60 MeV, while for ^{96}Nb we have 5894 1^+ states reaching energies of roughly 18 MeV. Since the exact energies of the intermediate states play an important role in the determination of the $2\nu\beta\beta$ NMEs, the excitation energies of the 1^+ states in ^{48}Sc were shifted such that the lowest-lying state is at the experimental energy of 2200 keV [11]. For ^{96}Nb no 1^+ states are known experimentally, so that the shell-model excitation energies were used. However, the paper by Thies et al. [30] suggests that the state at 694.6 keV could be the lowest 1^+ state. The branching-ratio calculations were thus repeated also for this scenario.

The phase-space integrals are taken from the work of Neacsu and Horoi [25]. The Q values are taken from [11] and are $Q_{\beta\beta}(^{48}\text{Ca}) = 4269.08(8)$ keV, $Q_\beta(^{48}\text{Ca}) = 279(5)$ keV, $Q_{\beta\beta}(^{96}\text{Zr}) = 3356.03(7)$ keV, and $Q_\beta(^{96}\text{Zr}) = 163.97(10)$ keV.

In the following we will first report on the computed results for the $2\nu\beta\beta$ NMEs of ^{48}Ca and ^{96}Zr and then extract effective values g_A^{eff} of the weak axial coupling based on comparisons with the measured $2\nu\beta\beta$ half-lives. These g_A^{eff}, listed in Table 1, are then, in turn, used to predict the β-decay branching ratios for transitions to the lowest 4^+, 5^+, and 6^+ states of ^{48}Sc and ^{96}Nb. This we consider to be a consistent approach since the $2\nu\beta\beta$ and β decays are low-momentum-exchange processes and thus the related axial couplings are expected to be quenched by a similar amount [26,27]. A further evidence comes from the very recent analyses of the electron-spectrum shape of the 4th-forbidden non-unique β^--decay transition $^{113}\text{Cd}(1/2^+) \to {}^{113}\text{In}(9/2^+)$ by the COBRA collaboration [31]. There values $g_A^{\text{eff}} \approx 0.91 - 0.95$ were obtained in three different theory frameworks. These values are consistent with those shown in Table 1.

The computed shell-model $2\nu\beta\beta$ NMEs are given in Table 1. For ^{48}Ca the shell-model calculation gives $|M_{2\nu}| = 0.0511$, which is 5% smaller than the value 0.0539 reported in [20]. The accumulation of the matrix element is in agreement with the previous results (see Fig. 1). The lowest 1^+ state is the most important, contributing an amount of 0.0454 to the total NME. The next dozen states are mostly constructive, adding up to a maximum value of 0.0847 of the NME, beyond which the states start to contribute destructively. When taking a closer look at the main constitution of this "bump" in the cumulative NME one notices that it emerges from the inclusion of both of the spin-orbit partners $0f_{7/2}$ and $0f_{5/2}$ in the calculations. The $0f_{7/2} - 0f_{7/2}$ contributions produce the rapid increase and the $0f_{7/2} - 0f_{5/2}$ contributions cause the fast decrease of the NME. Our cumulative NME agrees with the previous result when 50 intermediate states are used (reaching at about 9.4 MeV). The next approximately 150 states (reaching 13.4 MeV) add destructively to the cumulative NME bringing the NME to a value 0.0505. The 200th to 460th states (up to 16.9 MeV) add con-

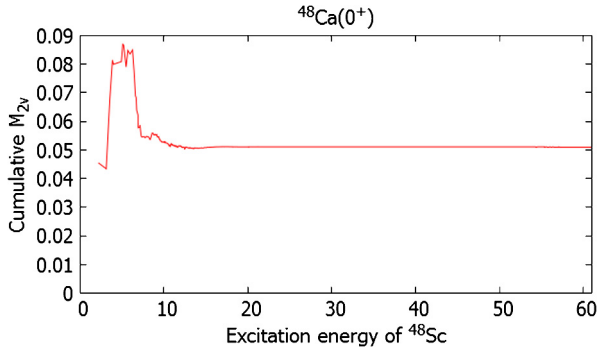

Fig. 1. Cumulative $2\nu\beta\beta$ NME $M_{2\nu}$ for ^{48}Ca as a function of excitation energy of the intermediate state in ^{48}Sc.

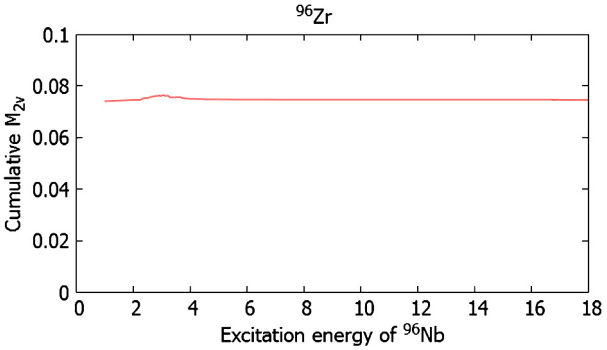

Fig. 2. Cumulative $2\nu\beta\beta$ NME $M_{2\nu}$ for ^{96}Zr as a function of excitation energy of the intermediate state in ^{96}Nb.

structively beyond which the cumulative matrix element tapers off to the final value 0.0511.

In the case of ^{96}Zr (see Fig. 2) there is a clear single-state dominance (SSD) [28,29], with the first excited state contributing an amount of 0.0747 to the total NME, while the sum of the other contributions is zero to three significant digits. This agrees with the measurement of Thies et al. [30] where extreme SSD was reported to be found in the $2\nu\beta\beta$ NME of ^{96}Zr in a high-resolution ^{96}Zr(^{3}He, t) experiment. Hence, our calculations confirm the experimental result of [30]. The accumulation for ^{96}Zr is very similar to the 48Ca case with the first 15 states adding constructively to 0.0765, beyond which the rest of the states contribute destructively. Beyond the first 100 states (7.5 MeV) the contributions are negligible.

Solving for g_A from equation (5) and using the experimental half-lives from [9,10], phase-space integrals from [25], and the present shell-model NMEs, we get the effective g_A values $g_A^{\rm eff} = 0.80 \pm 0.04$ for ^{48}Ca and $g_A^{\rm eff} = 1.04^{+0.03}_{-0.02}$ for ^{96}Zr. These values of $g_A^{\rm eff}$ are specific for the used model spaces and Hamiltonians. In the work of Barea et al. [35] a relation $g_A^{\rm eff} = 1.269 \times A^{-0.12}$ between the axial-vector coupling and the mass number A was found when analyzing the values of the $2\nu\beta\beta$ NMEs obtained in earlier calculations using the interacting shell model. Based on this, we would expect $g_A^{\rm eff} = 0.80$ for ^{48}Ca and $g_A^{\rm eff} = 0.73$ for ^{96}Zr. For calcium the values match perfectly, while for zirconium less quenching seems to be needed. However, the ^{96}Zr value seems to be consistent with the recent calculations on ^{130}Te and ^{136}Xe [36,37], where a value $g_A^{\rm eff} = 0.94$ was found, since we expect these heavier nuclei to require more g_A quenching than the lighter ^{96}Zr.

As mentioned earlier, the measurement of Thies et al. [30] suggests that the state at 694.6 keV in ^{96}Nb might be the first 1^+ state. If we repeat the calculations with this assumption, the total matrix element for ^{96}Zr decay is increased to 0.0854, which in turn gives $g_A^{\rm eff} = 0.97^{+0.03}_{-0.02}$ for ^{96}Zr.

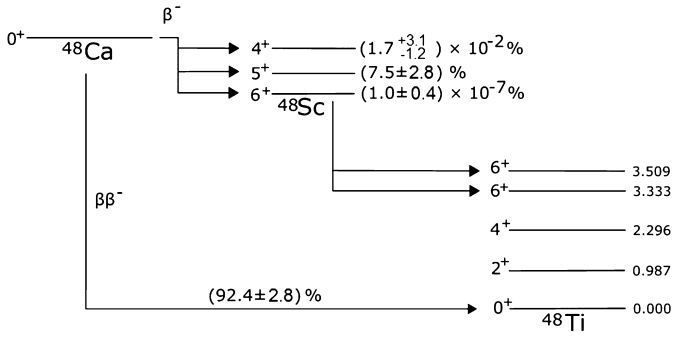

Fig. 3. Decay scheme of ^{48}Ca. Also indicated are our shell-model computed β-decay and $2\nu\beta\beta$-decay branching ratios.

At this point it should be made clear that the presently adopted valence spaces are not complete which is reflected in the effective values $g_A^{\rm eff}$ of Table 1. Furthermore, the valence-space truncations affect differently the ^{48}Ca and ^{96}Zr decays. For the ^{48}Ca decay we are able to include all spin-orbit partners but for the ^{96}Zr decay we are forced to leave out the proton $0g_{7/2}$ orbital (partner of the $0g_{9/2}$ orbital) and the neutron $0g_{9/2}$ orbital (partner of the $0g_{7/2}$ orbital) due to an excessive growth of the computational burden. This could affect the final value of the $2\nu\beta\beta$ NME and thus the corresponding value of $g_A^{\rm eff}$. In particular the β^+-side transitions could be affected as pointed out by Towner [32]. More insight into the problem of missing spin-orbit partners could be obtained by computing the $2\nu\beta\beta$ NME of ^{96}Zr by the use of the proton-neutron quasiparticle random-phase approximation (pnQRPA) [33]. Here the result depends very much on the value of the particle-particle strength parameter $g_{\rm pp}$ [34]. Performing pnQRPA calculations of the ^{96}Zr $2\nu\beta\beta$ NME within a reasonable interval of $g_{\rm pp}$ values indicates that the presently omitted spin-orbit partners have an effect in the pnQRPA calculations. These orbitals introduce small negative contributions to the first contribution which is positive and by far the largest one. This interference of the first contribution and the high-lying contributions can lead to a reduction of the $2\nu\beta\beta$ NME in the range of tens of per cent, depending on the value of $g_{\rm pp}$. Most likely something similar could be expected for the shell-model calculation, thus increasing the value of $g_A^{\rm eff}$ from the value given in Table 1 and altering the β-decay branching ratios given below. Since adding the spin-orbit partners affects also the β-decay strengths it is hard to predict how the branchings to β decays would be altered in the end.

The β transitions to the 4^+, 5^+, and 6^+ states in ^{48}Sc and ^{96}Nb are 4th-forbidden non-unique, 4th-forbidden unique and 6th-forbidden non-unique, respectively. A priori, without any calculations, one could predict that the 6th-forbidden non-unique β transition is much suppressed relative to the other two due to the much higher degree of forbiddenness that overwhelms the positive boost coming from the slightly larger Q value relative to the other two transitions. With less certainty one could predict that the NMEs of the two 4th-forbidden β transitions are on the same ball park and the difference in the Q value is most likely the decisive element in defining the branching between the two transitions. In the following we test these hypotheses by the shell-model calculations of the involved NMEs.

The β-decay and $2\nu\beta\beta$-decay branching ratios calculated for ^{48}Ca are indicated in Fig. 3. As expected, the $2\nu\beta\beta$ branch is clearly dominant with a $92.4 \pm 2.8\%$ branching. The β-decay branches to the $4^+, 5^+, 6^+$ states are $(1.7^{+3.1}_{-1.2}) \times 10^{-2}\%$, $7.5 \pm 2.8\%$ and $(1.0 \pm 0.4) \times 10^{-7}\%$. The branching to the 5^+ state therefore poten-

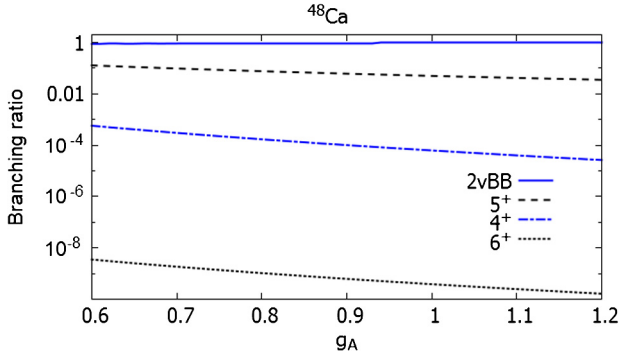

Fig. 4. Branching ratios of all the decay branches of ^{48}Ca as functions of g_A. The solid line represents the $2\nu\beta\beta$-decay branching and the dashed and dotted lines the β-decay branches. The β-decay branches are labeled by the spin-parity of the final state.

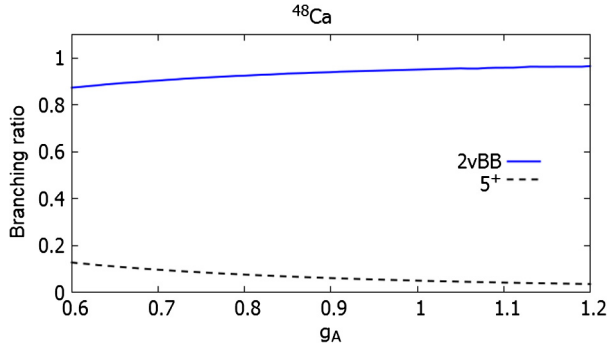

Fig. 5. Branching ratios of the two dominant branches of ^{48}Ca as functions of g_A.

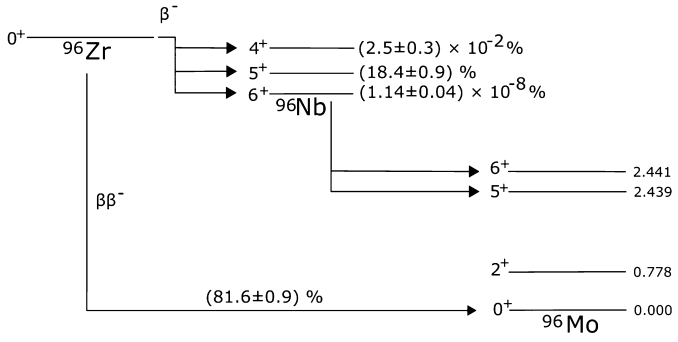

Fig. 6. Decay scheme of ^{96}Zr. Also indicated are our shell-model computed β-decay and $2\nu\beta\beta$-decay branching ratios.

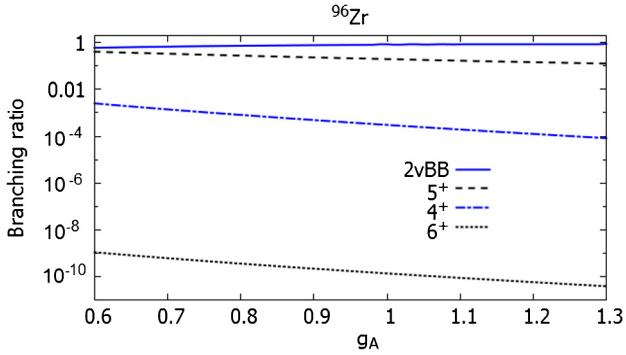

Fig. 7. Branching ratios of all the decay branches of ^{96}Zr as functions of g_A. The solid line represents the $2\nu\beta\beta$-decay branching and the dashed and dotted lines the β-decay branches. The β-decay branches are labeled by the spin-parity of the final state.

tially competes with the $2\nu\beta\beta$ branch in a significant way, as was pointed out in [6]. The decay to the 6^+ state is greatly hindered by the fact that it is sixth-forbidden. Based on the change in angular momentum, we would expect in general the decay to the 4^+ state be the fastest. However, in this case this branch is quite small due to the relatively small Q value. In the work of Haaranen et al. [6] the half-lives for the 4^+ and 6^+ states were reported for $g_A = 1.0$ and $g_A = 1.27$. The half-lives are shortened from 3.97×10^{23} yr to $(3.47 \pm 0.09) \times 10^{23}$ yr for the 4^+ state and from 6.39×10^{28} to 5.61×10^{28} yr, when our $2\nu\beta\beta$-determined $g_A = 0.80 \pm 0.04$ is adopted instead of $g_A = 1.00$. The unique-forbidden 5^+ branch is 50–60% stronger than suggested in [6], since the presently adopted heavier quenching of g_A affects stronger the $2\nu\beta\beta$ branch. The small differences in the half-lives compared to the calculations in [6] are due to the inclusion of the next-to-leading-order NMEs and kinematic factors in the present study as well as the updated Q value, which is 1 keV larger than used in the study of [6]. As g_A is quenched more, the significance of all the β-decay branches increases. For the unique 5^+ transition the g_A dependence of the decay half-life is well known and roughly g_A^{-2} but for the non-unique transitions this is not the case due to the more complex structure of the shape factor. The uncertainties related to the branching to the 4^+ state are especially large due to the fact that the 5 keV uncertainty makes a large percentage of the 26.65 keV Q value. An accurate measurement of the Q value would decrease the uncertainties significantly and thus would be desirable.

The g_A dependence of all the decay branchings from ^{48}Ca is studied in Fig. 4. As can be seen the dependence on the value of g_A is similar for the β branchings and they decrease substantially with increasing value of g_A. At the same time the $2\nu\beta\beta$-decay branching increases slowly towards one, as can be better seen in Fig. 5 where only the $2\nu\beta\beta$ and 4th-forbidden-unique decay branchings are plotted as functions of g_A. For reasonable values of g_A the β branching to the 5^+ state is always below 20%.

The computed branching ratios for ^{96}Zr are presented in Fig. 6. Like for ^{48}Ca the $2\nu\beta\beta$ branch for ^{96}Zr is the largest one at (81.6 ± 0.9)% but the dominance is not as significant as in the ^{48}Ca case. The branching ratios for the β-decay transitions are qualitatively similar to calcium case with 4^+ state having a branching ratio of $(2.5 \pm 0.3) \times 10^{-2}$%, the unique 5^+ branch (18.4 ± 0.9)%, and the ground-state-to-ground-state branch being by far the weakest at $(1.14 \pm 0.04) \times 10^{-8}$%. Using the computed β-decay half-lives reported in the previous shell-model study [8] of the decay of ^{96}Zr we can extract the corresponding branching ratios of 2.6×10^{-2}%, 17.6%, and 1.21×10^{-8}% in line with the presently determined branchings. The non-unique β branches in the present study are slightly smaller than those obtained in [8] but the branching to the 5^+ state is notably stronger than expected based on Ref. [8]. This seems to confirm that the β decay might be up to 2.3 times faster than predicted by the older QRPA calculations in [7].

With the assumption that the first 1^+ state in ^{96}Nb is at 694.6 keV, the branching ratios remain largely unchanged amounting to (83.3 ± 0.8)%, $(3.0 \pm 0.4) \times 10^{-2}$%, (16.7 ± 0.9)%, and $(1.19 \pm 0.15) \times 10^{-8}$% for the $2\nu\beta\beta$, 4^+, 5^+, and 6^+ decays respectively.

The dependence of all the ^{96}Zr decay branchings on g_A is studied in Fig. 7. As can be seen, a similar g_A dependence as in the case of ^{48}Ca is recorded. A closer look at the two leading branchings to the $2\nu\beta\beta$ and 4th-forbidden-unique decays, depicted in Fig. 8, indicates that their g_A dependence is much stronger than in the case of ^{48}Ca. In the ^{96}Zr case the β branching to the 5^+ state can reach values up to 40% for low values of g_A. Such large branchings could be measurable in dedicated experiments sometime in the future.

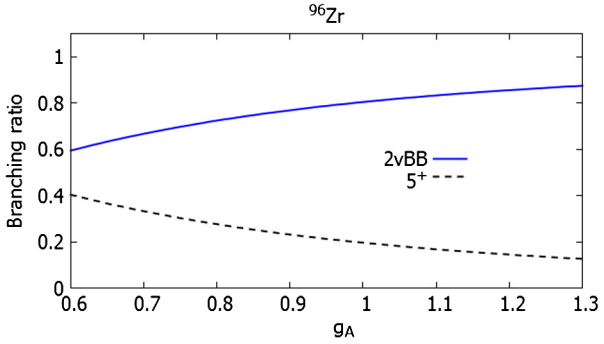

Fig. 8. Branching ratios of the two dominant branches of ^{96}Zr as functions of g_A.

In this Letter the $2\nu\beta\beta$ matrix elements and single-β-decay branching ratios were calculated for ^{48}Ca and ^{96}Zr in the framework of the interacting nuclear shell model using large single-particle valence spaces and matching well-tested many-body Hamiltonians. For ^{48}Ca a $2\nu\beta\beta$ matrix element $M_{2\nu} = 0.0511$ was obtained, which is 5.5% smaller than the value of 0.0539 reported in the previous calculation of Horoi et al. [20]. For ^{96}Zr this was the first large-scale shell-model calculation yielding a value of $M_{2\nu} = 0.0747$ using the shell model excitation energies and $M_{2\nu} = 0.0854$ when the first 1^+ state is assumed to be at 694.6 keV in ^{96}Nb, as suggested by the high-resolution ^{96}Zr(^{3}He, t) experiment of Thies et al. [30]. An extreme single-state dominance was found thus verifying the result of the mentioned charge-exchange experiment [30]. Using these matrix elements, combined with measured values of $2\nu\beta\beta$ half-lives, effective quenched values of the weak axial coupling g_A were extracted to be further used in the analyses of the β-decay branchings. In this way a consistent treatment of both the $2\nu\beta\beta$ decay and the competing β decays was achieved.

The $2\nu\beta\beta$-decay and β-decay branching ratios were studied for their g_A dependence and the total branchings to the β channels were determined to be $(7.5 \pm 2.8)\%$ for ^{48}Ca and $(18.4 \pm 0.09)\%$ for ^{96}Zr using the mentioned consistent effective values of g_A. These branchings are in both cases larger than predicted in previous studies and could be large enough to be detected in underground experiments in the near future. The bulk of the uncertainty related to the ^{48}Ca branching ratios is due to the imprecise knowledge of the Q values. Therefore, a precise measurement of the ground-state-to-ground-state Q value for this case would be desirable.

Acknowledgements

This work has been partially supported by the Academy of Finland under the Academy project no. 318043. J.K. acknowledges the financial support from Jenny and Antti Wihuri Foundation.

References

[1] H. Ejiri, J. Suhonen, K. Zuber, Phys. Rep. 797 (2019) 1.
[2] A. Poves, R.P. Bahukutumbi, K. Langanke, P. Vogel, Phys. Lett. B 361 (1995) 1.
[3] J. Suhonen, J. Phys. G, Nucl. Part. Phys. 19 (1993) 139.
[4] A. Balysh, A. De Silva, V.I. Lebedev, K. Lou, M.K. Moe, et al., Phys. Rev. Lett. 77 (1996) 5186.
[5] A. Bakalyarov, A. Balysh, A. Barabash, C. Briançon, V. Brudanin, et al., Nucl. Phys. A 700 (2002) 17.
[6] M. Haaranen, M. Horoi, J. Suhonen, Phys. Rev. C 89 (2014) 034315.
[7] H. Heiskanen, M.T. Mustonen, J. Suhonen, J. Phys. G, Nucl. Part. Phys. 34 (2007) 837.
[8] M. Alanssari, D. Frekers, T. Eronen, L. Canete, J. Dilling, et al., Phys. Rev. Lett. 116 (2016) 072501.
[9] R. Arnold, C. Augier, A.M. Bakalyarov, J.D. Baker, A.S. Barabash, et al., NEMO-3 Collaboration, Phys. Rev. D 93 (2016) 112008.
[10] J. Argyriades, R. Arnold, C. Augier, J. Baker, A. Barabash, et al., Nucl. Phys. A 847 (2010) 168.
[11] National Nuclear Data Center, Brookhaven National Laboratory, www.nndc.bnl.gov.
[12] A.S. Barabash, R. Gurriarán, F. Hubert, P. Hubert, J.L. Reyss, J. Suhonen, V.I. Umatov, J. Phys. G, Nucl. Part. Phys. 22 (1996) 487.
[13] H. Behrens, W. Bühring, Electron Radial Wave Functions and Nuclear Beta Decay, Oxford University Press, Clarendon, Oxford, 1982.
[14] M. Haaranen, J. Kotila, J. Suhonen, Phys. Rev. C 95 (2017) 024327.
[15] J. Suhonen, O. Civitarese, Phys. Rep. 300 (1998) 123.
[16] J.C. Hardy, I.S. Towner, V. Koslowsky, E. Hagberg, H. Schmeing, Nucl. Phys. A 509 (1990) 429.
[17] M. Haaranen, P.C. Srivastava, J. Suhonen, Phys. Rev. C 93 (2016) 034308.
[18] J. Kostensalo, M. Haaranen, J. Suhonen, Phys. Rev. C 95 (2017) 044313.
[19] B.A. Brown, W.D.M. Rae, Nucl. Data Sheets 120 (2014) 115.
[20] M. Horoi, S. Stoica, B.A. Brown, Phys. Rev. C 75 (2007) 034303.
[21] M. Honma, T. Otsuka, B.A. Brown, T. Mizusaki, Phys. Rev. C 69 (2004) 034335.
[22] M. Honma, T. Otsuka, B.A. Brown, T. Mizusaki, Eur. Phys. J. A 25 (2005) 499.
[23] H. Mach, E.K. Warburton, R.L. Gill, R.F. Casten, J.A. Becker, B.A. Brown, J.A. Winger, Phys. Rev. C 41 (1990) 226.
[24] D.H. Gloeckner, Nucl. Phys. A 253 (1975) 301.
[25] A. Neacsu, M. Horoi, Adv. High Energy Phys. 2016 (2016) 7486712.
[26] J. Suhonen, Front. Phys. 5 (2017) 55.
[27] J. Suhonen, J. Kostensalo, Front. Phys. 7 (2019) 29.
[28] O. Civitarese, J. Suhonen, Phys. Rev. C 58 (1998) 1535.
[29] O. Civitarese, J. Suhonen, Nucl. Phys. A 653 (1999) 321.
[30] J.H. Thies, P. Puppe, T. Adachi, M. Dozono, H. Ejiri, et al., Phys. Rev. C 86 (2012) 054323.
[31] L. Bodenstein-Dresler, Y. Chu, D. Gehre, C. Gössling, A. Heimbold, et al., COBRA Collaboration, Phys. Lett. B 800 (2020) 135092.
[32] I.S. Towner, Nucl. Phys. A 444 (1985) 402.
[33] J. Suhonen, O. Civitarese, J. Phys. G, Nucl. Part. Phys. 39 (2012) 085105.
[34] O. Civitarese, A. Faessler, T. Tomoda, Phys. Lett. B 194 (1987) 11.
[35] J. Barea, J. Kotila, F. Iachello, Phys. Rev. C 87 (2013) 014315.
[36] A. Neacsu, M. Horoi, Phys. Rev. C 91 (2015) 024309.
[37] M. Horoi, A. Neacsu, Phys. Rev. C 93 (2016) 024308.